Microwave and Wireless Technologies Series

Low-cost Smart Antennas

Qi Luo | Steven (Shichang) Gao | Wei Liu | Chao Gu

WILEY

Low-cost Smart Antennas

Microwave and Wireless Technologies Series

Series Editor, Professor Steven (Shichang) Gao, Chair of RF and Microwave Engineering, and the Director of Postgraduate Research at School of Engineering and Digital Arts, University of Kent, UK.

Microwave and wireless industries have experienced significant development during recent decades. New developments such as 5G mobile communications, broadband satellite communications, high-resolution earth observation, the Internet of Things, the Internet of Space, THz technologies, wearable electronics, 3D printing, autonomous driving, artificial intelligence etc. will enable more innovations in microwave and wireless technologies. The Microwave and Wireless Technologies Book Series aims to publish a number of high-quality books covering topics of areas of antenna theory and technologies, radio propagation, radio frequency, microwave, millimetre-wave and THz devices, circuits and systems, electromagnetic field theory and engineering, electromagnetic compatibility, photonics devices, circuits and systems, microwave photonics, new materials for applications into microwave and photonics, new manufacturing technologies for microwave and photonics applications, wireless systems and networks.

Low-cost Smart Antennas

Qi Luo, and Steven (Shichang) Gao
University of Kent, Canterbury, UK

Wei Liu
University of Sheffield, Sheffield, UK

Chao Gu
University of Kent, Canterbury, UK

WILEY

This edition first published 2019

Registered Offices
John Wiley & Sons, Inc., 111 River Street, Hoboken, NJ 07030, USA
John Wiley & Sons Ltd, The Atrium, Southern Gate, Chichester, West Sussex, PO19 8SQ, UK

Editorial Office
The Atrium, Southern Gate, Chichester, West Sussex, PO19 8SQ, UK

For details of our global editorial offices, customer services, and more information about Wiley products visit us at www.wiley.com.

Wiley also publishes its books in a variety of electronic formats and by print-on-demand. Some content that appears in standard print versions of this book may not be available in other formats.

Library of Congress Cataloging-in-Publication Data

Names: Luo, Qi, 1982- author. | Gao, Steven (Shichang), author. | Liu, Wei, 1974- author. | Gu, Chao, 1986 Sept. 24- author.
Title: Low-cost smart antennas / Qi Luo, Steven (Shichang) Gao, Wei Liu, and Chao Gu.
Description: First edition. | Hoboken, NJ : Wiley, [2019] | Series: Microwave and wireless technologies series | Includes bibliographical references and index. |
Identifiers: LCCN 2018042667 (print) | LCCN 2018050919 (ebook) | ISBN 9781119422792 (Adobe PDF) | ISBN 9781119422877 (ePub) | ISBN 9781119422778 (hardcover)
Subjects: LCSH: Adaptive antennas.
Classification: LCC TK7871.67.A33 (ebook) | LCC TK7871.67.A33 L86 2019 (print) | DDC 621.3841/35–dc23
LC record available at https://lccn.loc.gov/2018042667

Cover Design: Wiley
Cover Images: Abstract texture © AboutnuyLove/iStock.com, Vector mockup © ExtraDryRain/iStock.com, SUV © Henrik5000/iStock.com, Airplane © lvcandy/iStock.com, Broadcast satellite © Madmaxer/iStock.com, Cellular camera © Flamell/iStock.com, High-speed train © Nerthuz/iStock.com, Low-cost smart antenna courtesy of the authors

Set in 10/12pt WarnockPro by SPi Global, Chennai, India

10 9 8 7 6 5 4 3 2 1

Contents

Preface

Smart antennas are antennas with smart signal-processing algorithms that can electronically reconfigure radiation patterns so that the maximum radiation is formed towards the desired directions while nulls are formed towards interfering sources. It is a key technology for many wireless systems, such as satellite communications, terrestrial mobile communications, inter-satellite links, radio-frequency identification, wireless power transmission, wireless local area networks, global navigation satellite systems, radars, remote sensing, and direct broadcast satellite television reception systems. Traditional smart antennas using phased arrays or digital beamforming adaptive arrays are rather complicated in structure, bulky, power hungry, and costly. For commercial applications, it is important to reduce the size, mass, power consumption, and cost of smart antennas. Recent decades have seen lots of progress in research and development in the field of low-cost smart antennas. It is foreseen that low-cost smart antennas will be widely implemented in the smart city, fifth-generation and future generations of mobile communications, smart homes, satellite communication on the move, the Internet of Things, the Internet of Space, and autonomous vehicles.

So far, most books on smart antennas have mainly focused on signal-processing algorithms, and there are few books specialising in antennas and the radio frequency (RF) hardware of smart antennas. The purpose of this book is to address practical antenna design and RF engineering issues in low-cost smart antennas by presenting various techniques for designing and implementing low-cost smart antennas. These techniques include the electronically steerable parasitic array radiator, the reconfigurable frequency selective surface, pattern-reconfigurable reflectarrays and transmitarrays, compact multiple-input multiple-output antenna systems, and the use of low-cost beamforming networks. Each topic is addressed with both theoretical explanations and practical design examples. Each chapter contains basic principles, design techniques, a detailed review of state-of-the-art development, and practical case studies to illustrate how to design low-cost smart antennas step by step. To provide readers with some basics of beamforming algorithms and their applications in smart antennas, Chapter 2 discusses the basic principles of beamforming and introduces some representative beamforming methods and algorithms for smart antennas. A review of the particular area of low-cost

adaptive beamforming is also presented in this chapter, including hybrid beamforming and robust adaptive beamforming.

This book contains fundamental theory, many practical design examples, advanced design techniques, and case studies, thus it is a useful reference for people from both industry and academia who are interested in smart antennas. The references listed in each chapter offer additional sources of data for readers.

Acknowledgement

The authors would like to thank Sandra Grayson, Louis Manohar, and Kanchana Kathirvelu of Wiley for their help and guidance during the preparation of this book.

Dr Qi Luo would like to express his appreciation and gratitude to his family for their encouragement, understanding, and patience during the writing of this book. He also would like to express his thanks for technical discussions to the members of the antenna research group at the University of Kent, UK.

Professor Steven (Shichang) Gao would like to thank his wife Jun Li and his daughter Karen Yu Gao for their great understanding and support during the period of book writing. He also would like to thank all of his current and former students and research collaborators who contributed to the research work on low-cost smart antennas. In particular, thanks to Dr Haitao Liu, Dr Long Zhang, Mr Hang Xu, Dr Fan Qin, Mr Mingtao Zhang, Dr Benito Sanz, Professor Ted Parker, Dr Hanyang Wang, Dr Hai Zhou, Professor Xuexia Yang, Professor Yingzeng Yin, Professor Yongchang Jiao, Professor Ying Liu, Associate Professor Jianzhou Li, Professor Gao Wei, Professor Jiadong Xu, Professor Luigi Boccia, and Professor Amendola Giandomenico who made important contributions into the research on low-cost smart antennas.

Dr Wei Liu would like to thank all former and current members of his research group for their hard work and creativity, and especially those who joined his group at the early stage of his career. In particular, some of the work presented in the book is closely related to the research carried out by Lei Zhang, Qiu Bo, and Craig Miller.

Dr Chao Gu would like to thank Simon Jakes for the help he provided in prototyping the antennas. He also wishes to express his heartfelt gratitude to his wife, Dr Lu Bai, for her support and unwavering belief.

Parts of the research work presented in this book were supported by EPSRC grants EP/N032497/1, EP/P015840/1, and EP/S005625/1.

List of Abbreviations

2D-FFT	Two-dimensional fast Fourier transform
ABF	Analogue beamforming
AC	Alternating current
A/D	Analogue/digital
ADC	Analogue-to-digital converter
AF	Array factor
AFR	Array-fed reflector
AFSS	Active frequency selective surface
AMC	Artificial magnetic conductor
AOA	Angle of arrival
AR	Axial ratio
AWGN	Additive white Gaussian noise
BFN	Beamforming network
BP	Beam pattern
CAFSS	Cylindrical active frequency selective surface
CCC	Cross-correlation coefficient
CMA	Constant modulus algorithm
CP	Circularly polarised
DAC	Digital-to-analogue converter
dB	Decibels
DBF	Digital beamforming
DC	Direct current
DDC	Digital down-converter
DGS	Defect ground system
DOA	Direction of arrival
DSP	Digital signal processor
EBG	Electromagnetic band gap
ECC	Envelope correlation coefficient
ECM	Equivalent circuit method
EM	Electromagnetic
ESPAR	Electronically steerable parasitic array radiator
FBR	Front-to-back ratio
FDTD	finite difference time domain
FEM	finite element method
FIR	Finite impulse response

FM-ESPAR	Folded monopole ESPAR
FOM	Figures of merit
FP	Fabry–Perot
FPGA	Field-programmable gate array
FSK	Frequency shift keying
FSS	Frequency selective surface
GCPW	Grounded coplanar waveguide
GNSS	Global navigation satellite system
GPIO	General purpose input/output
GPS	Global positioning system
HIS	High impedance surface
HPBW	Half-power beamwidth
IF	Intermediate frequency
ILA	Inverted-L antenna
INR	Interference-to-noise ratio
LAN	Local-area network
LC	Inductor-capacitor
LCMV	Linearly constrained minimum variance
LCP	Liquid crystal polymer
LHCP	Left-hand circularly polarised
LMS	Least mean squares
LO	Local oscillator
LQI	Link quality indicator
LS	Least squares
LTCC	Low temperature co-fired ceramic
LTE	Long-term evolution
MCU	Micro control unit
MEMS	Microelectromechanical systems
MIMO	Multiple-input multiple-output
mm-wave	Millimetre-wave
MPR	Metamaterial polarisation-rotator
MSR	Mainlobe to sidelobe ratio
MTM	Metamaterial
MUSIC	MUltiple SIgnal Classification
NMSE	Normalised mean square error
PCB	Printed circuit board
PBG	Photonic bandgap
PER	Package error rate
PFGA	Field-programmable gate array
PIFA	Planar inverted-F antenna
PRS	Partially reflective surface
PSK	Phase shift keying
QPSK	Quadrature phase shift keying
RF	Radio frequency
RHCP	Right-hand circularly polarised
RLC	Resistor-inductor-capacitor
RLS	Recursive least squares

SAR	Specific absorption rate
SDL	Sensor delay line
SINR	Signal to interference plus noise ratio
SIW	Substrate-integrated waveguide
SLL	Sidelobe level
SMA	SubMiniature version A
SNR	Signal-to-noise ratio
SOI	Signal of interest
SP3T	Single pole triple throw
SRF	Self-resonant frequency
SRR	Split-ring resonator
TA	Transmitarray
TARC	Total active reflection coefficient
TDL	Tapped delay line
TE	Transverse electric
TM	Transverse magnetic
T/R	Transmit/receive
TTL	Transistor–transistor logic
ULAs	Uniform linear arrays
USB	Universal serial bus
VCO	Voltage-controlled oscillator
VNA	Vector network analyser
VSWR	Voltage standing wave ratio
WiMAX	Worldwide interoperability for microwave access
WLAN	Wireless local-area network

1

Introduction to Smart Antennas

1.1 Introduction

Smart antennas, also known as intelligent antennas or adaptive arrays, are a key technology for advanced wireless systems, such as satellite communications, inter-satellite links, radars, sensors, mobile communications (5G and beyond), wireless local area networks, global navigation satellite systems, and wireless power transfer. One of the most important features of smart antennas is electronic beam scanning or switching. Smart antennas enable wireless systems to achieve optimum performance and increase channel throughput by electronically steering maximum radiation towards the desired directions while forming nulls against interfering sources.

The adaptive array is 'smart' because it has signal processing units with smart signal processing algorithms. Recent years have seen the development of efficient algorithms for direction of arrival (DOA) estimation and adaptive beamforming. Algorithms for adaptive beamforming include the classical least mean squares (LMS) type algorithm, constant modulus algorithm (CMA) etc. Traditional smart antennas are, however, complicated in structure, bulky in size, and costly. Thus, it is highly desirable to reduce the size, mass, power consumption, and cost of smart antennas.

Generally speaking, smart antennas can be divided into three components: the antenna, the beamforming network (BFN), and the signal processing unit. It is believed that radio frequency (RF) designs such as the architecture design and configurations of antenna and BFN play an important role in determining the overall cost of a smart antenna. A good example is the phased array in which each of the antenna elements has its own RF chain, and the number of active antenna elements determines the number of transmit/receive (T/R) modules and the complexity of the BFN. An active phased array with 1000 antenna elements typically requires 1000 RF phase shifters, 1000 RF transceivers, and a highly complicated BFN, resulting in large size, heavy weight, high power consumption, and high cost. For civilian applications, it is crucial to develop low-cost smart antennas. Here low-cost smart antennas refer to antenna systems which can achieve electronic beam scanning, multiple beams or electronic beam-switching, and have significantly lower cost compared to traditional smart antennas such as phased arrays or digital beamforming smart antennas. Low-cost smart antennas can be achieved by designing innovative antenna system architectures that require a

Low-cost Smart Antennas, First Edition. Qi Luo, Steven (Shichang) Gao, Wei Liu, and Chao Gu.

significantly reduced number of T/R modules and RF phase shifters, or simplified BFNs with low-cost beamforming algorithms.

This book focuses on the RF design of smart antennas from the aspect of the array antenna, BFN, and related beamforming algorithms. The main purpose of the book is to present the techniques of RF designs of low-cost smart antennas as well as the hardware implementations of the antenna and the BFN. As multiple-input multiple-output (MIMO) antennas are often regarded as one type of smart antennas, compact-size MIMO antennas are included as one special type of low-cost smart antennas in this book. Due to the importance of beamforming algorithms for smart antennas, one chapter on beamforming algorithms is also included and many examples are discussed.

This chapter will provide an introduction to the fundamental concepts of antennas, array antennas, and smart antennas, laying a foundation for the following chapters. Configurations of smart antennas are also explained and discussed.

1.2 Antenna Fundamentals

In this section, some fundamental parameters of antennas are briefly presented, including input impedance, bandwidth, radiation pattern, polarisation, efficiency, and gain. These are key parameters for an antenna and are critical for the radiation performance of smart antennas.

1.2.1 Antenna Impedance and Bandwidth

The input impedance of the antenna is defined as the ratio of voltage to current at the terminal of the antenna. It is the ratio of the voltage to current or the ratio of the appropriate components of the electric to magnetic fields at the feed point [1]. The impedance of the antenna is usually a complex number and it is frequency dependent. It can be expressed as

$$Z_A = R_A + jX_A \tag{1.1}$$

where Z_A, R_A and X_A represent the antenna impedance, antenna resistance, and antenna reactance at the terminal of the antenna, respectively. The antenna resistance includes the radiation resistance (R_r) and the loss resistance (R_L) of the antenna

$$R_A = R_r + R_L \tag{1.2}$$

The radiation resistance is related to the power radiated by the antenna, and the loss resistance is associated with the power dissipated in the antenna due to the losses from the dielectric material and conductor. For a multi-port antenna, as a result of the mutual impedance between different ports, the input impedance of the antenna becomes [2]

$$Z_{A,i} = V_i/I_i = Z_{ii} + \sum_{j \neq i} Z_{ij} I_j / I_i \tag{1.3}$$

where $Z_{A,i}$ represents the input impedance at port i, Z_{ii} is the self-impedance of the i_{th} port, Z_{ij} is the mutual impedance between ports i and j, and I represents the current at the port of the antenna. As shown in Equation 1.3, the input impedance at port i is related to the excitations from other ports through the mutual impedance. Ideally, if

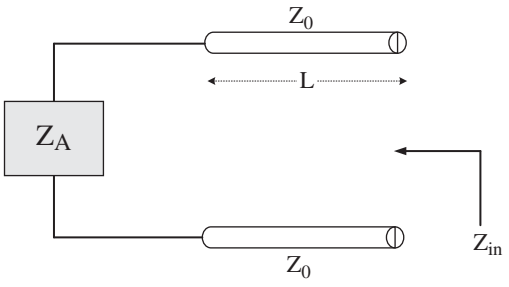

Figure 1.1 The equivalent circuit of the input impedance of the antenna with transmission line.

the mutual impedance is very small, the input impedance of each port is independent of the excitations of other ports. It is required that the antenna is impedance matched to the transmission line otherwise the antenna cannot radiate efficiently. As shown in Figure 1.1, when the antenna is terminated with a transmission with the impedance Z_0 and length L, the input impedance is

$$Z_{in} = Z_0 \frac{Z_A + jZ_0 \tan(L/\lambda)}{Z_0 + jZ_A \tan(L/\lambda)} \tag{1.4}$$

where λ is the wavelength in free space.

Figure 1.2 shows the input impedance of a typical probe-fed rectangular patch antenna. This patch has resonance at 9.75 GHz and the feeding coaxial cable has impedance of 50 Ω. This patch is printed on a 1.57 mm thick RT/Duroid 5880 substrate ($\varepsilon_r = 2.2$). As shown in Figure 1.2, at the resonance of the antenna the imaginary part of the input impedance is close to zero while the real part of the input impedance is close to 50 Ω. The reflection coefficient of the antenna is defined as

$$\Gamma = \frac{Z_{in} - Z_0}{Z_{in} + Z_0} \tag{1.5}$$

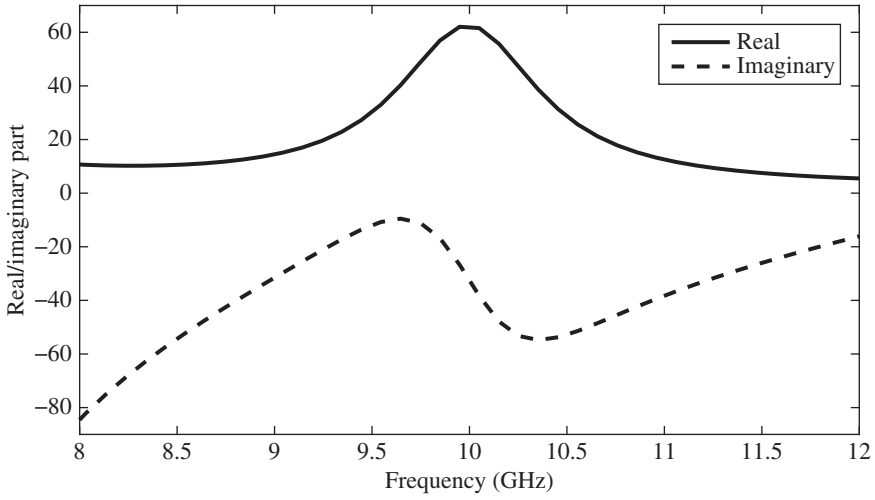

Figure 1.2 The input impedance of a typical probe-fed square patch antenna.

The concept of voltage standing wave ratio (VSWR) is introduced as a measure to show how well the antenna is matched. It is defined as the ratio of the maximum voltage (V_{max}) to the minimum voltage (V_{min}) in standing wave pattern along the transmission line. It is related to the reflection coefficient by

$$VSWR = \frac{V_{max}}{V_{min}} = \frac{1 + |\Gamma|}{1 - |\Gamma|} \tag{1.6}$$

As shown in Equation 1.6, VSWR is a real number that is always greater than or equal to 1. A VSWR of 1 indicates that there is no mismatch loss, while higher values of VSWR imply that there is large mismatch loss. Another parameter that can be used to quantise the matching of the antenna is return loss, which is defined as the ratio of rejected power against the input power to the antenna port. It is specified in decibels (dB) and is expressed as

$$RL = -20 \log |\Gamma| = -20 \log \left(\frac{VSWR - 1}{VSWR + 1} \right) \tag{1.7}$$

Another parameter that is equivalent to the return loss is the amplitude of the reflection coefficient |S11|. The |S11| represents how much power is reflected from the antenna. Generally speaking, the bandwidth of the antenna is defined as the frequency range where the return loss is larger than 10 dB ($|S11| < -10$ dB) or the VSWR is smaller than 2. In some applications, such as the mobile phone devices, the bandwidth of the antenna is defined as return loss larger than 6 dB while in base station application it is always desirable to have the return loss larger than 15 dB. Figure 1.3 shows the return loss and VSWR of the patch antenna presented in Figure 1.2. The 10 dB return loss bandwidth of the patch is approximately 5.8% at the central frequency of 9.75 GHz.

1.2.2 Radiation Patterns and Efficiency

The radiation pattern of the antenna shows the distribution of the radiated power in the far-field. It is defined as 'a mathematical function or a graphical representation of the

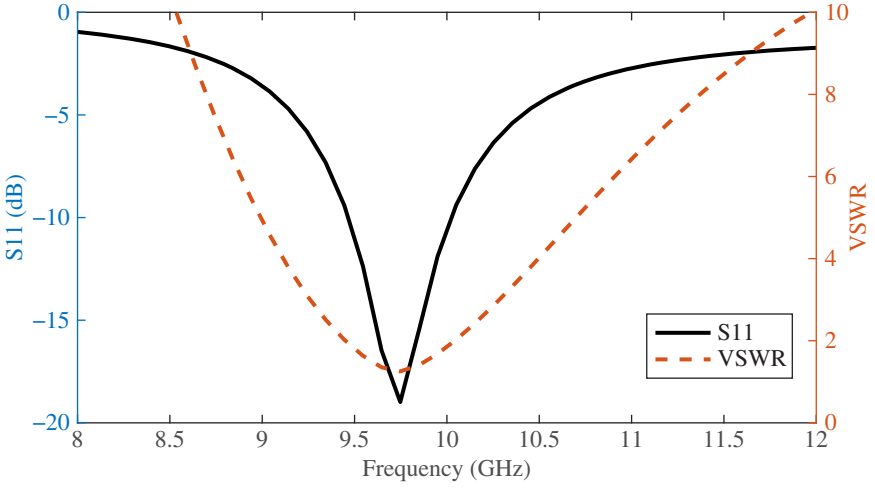

Figure 1.3 The return loss and VSWR of the patch antenna.

radiation properties of the antenna as a function of space coordinates' [1]. The power varies as a function of the angles that are observed in the far-field region of the antenna. In the far-field region, the radiation pattern does not change with distance. The far-field is defined as

$$R > \frac{2D^2}{\lambda} \tag{1.8}$$

$$R >> \lambda \tag{1.9}$$

$$R >> D \tag{1.10}$$

where D is the maximum dimension of the antenna and λ is the free space wavelength. The reactive near-field is the region that is close to the antenna. In this region, the electrical and magnetic fields are often complicated and are difficult to measure. This region is defined as

$$R < 0.62\sqrt{\frac{D^3}{\lambda}} \tag{1.11}$$

Between the far-field and reactive near-field region is the radiative near-field, which is also referred to as the Fresnel region. In this region there are no reactive field components from the antenna and the radiating fields begin to emerge. Figure 1.4 illustrates these regions of the antenna.

Figure 1.5 shows the far-field radiation patterns of some typical antennas. The directivity (D) is defined as the radiated power per unit solid angle compared to what would be received by an isotropic radiator [3]. As shown in Figure 1.5, different types of antenna have different directivity. The microstrip patch normally has a broad radiation pattern with moderate directivity. The dipole has an omnidirectional radiation pattern with typical gain of 2.3 dBi. The radiation pattern of the horn antenna has higher directivity. The directivity of the antenna can be increased by using an array antenna, as shown in Figure 1.5d.

The half-power beamwidth (HPBW) of an antenna is an important parameter for many applications, such as the base station antenna. It shows the angular range where

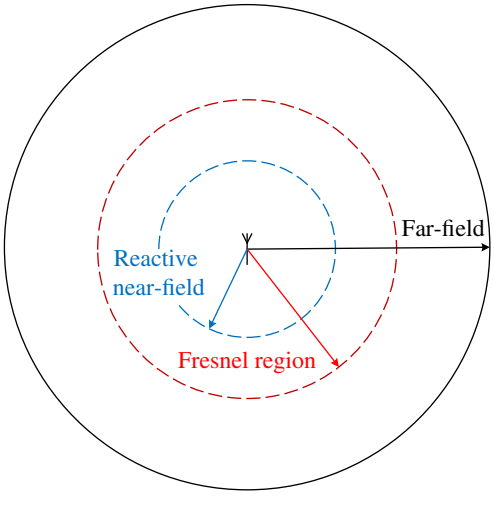

Figure 1.4 The different regions of the antenna field.

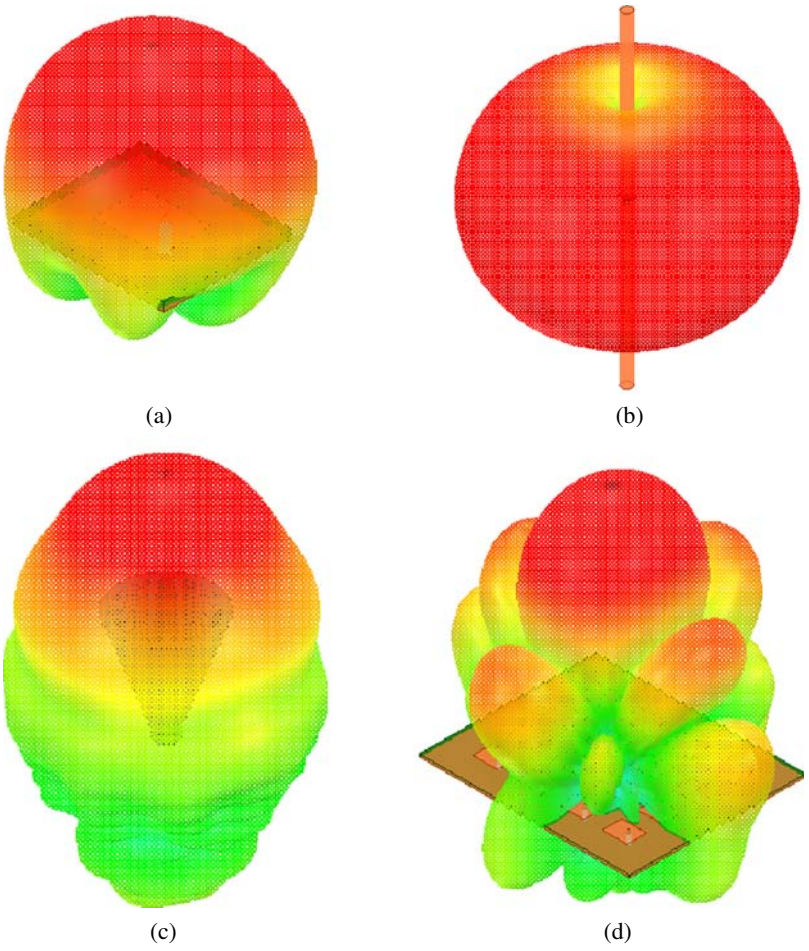

Figure 1.5 The radiation patterns of some typical antennas: (a) microstrip patch, (b) dipole antenna, (c) circular horn, and (d) microstrip array.

the radiated power has dropped by 50%. When plotting the radiation pattern in dB scale, the HPBW is where the power is reduced by 3 dB. Figure 1.6 shows an example of a directional radiation pattern that is plotted as the radiated power in dB versus the elevation angle (θ). High-directivity antennas always have a narrow HPBW, which can be seen from Figure 1.5.

The directivity of the antenna is calculated by

$$D(\phi, \varphi) = \frac{r^2 \frac{1}{2} Re[E \times H^*]}{P_{rad}/4\pi} \tag{1.12}$$

where P_{rad} is the radiated power. For a directional antenna, the directivity of the antenna can be estimated by [1]

$$D_0 \simeq \frac{4\pi(180/\pi)^2}{\theta_{1d}\theta_{2d}} = \frac{41253}{\theta_{1d}\theta_{2d}} \tag{1.13}$$

where θ_{1d} and θ_{2d} are the HPBW in two orthogonal planes.

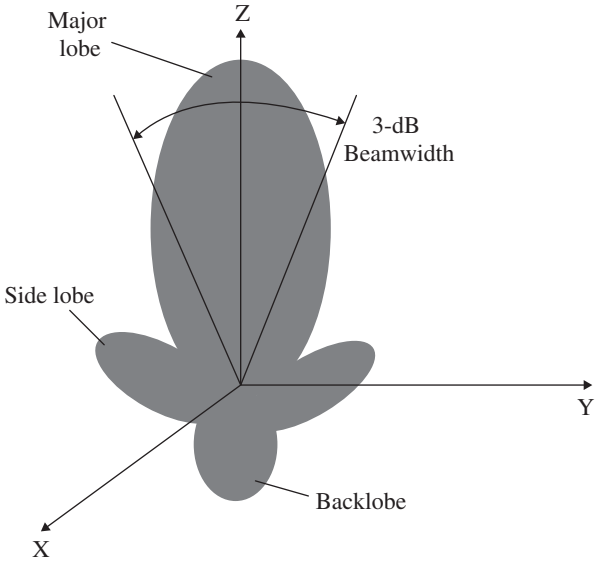

Figure 1.6 Illustration of the HPBW and the lobes of the antenna.

The gain of the antenna (G) is

$$G(\phi, \varphi) = \eta D(\phi, \varphi) \tag{1.14}$$

where η is the radiation efficiency of the antenna. The radiation efficiency describes how much input power is radiated from the antenna and is

$$\eta = \frac{P_{rad}}{P_{in}} \tag{1.15}$$

where P_{in} is the input power and P_{rad} is the radiated power. It is always desirable to have high-efficiency antennas; however, there are always some losses associated with the antenna, such as mismatching, dielectric loss, and conductor loss. The overall efficiency can be written as [1]

$$\eta = \eta_r \eta_c \eta_d \tag{1.16}$$

where η_r is the mismatching efficiency, η_c is the conduction efficiency, and η_d is the dielectric efficiency. The η_c and η_d are related to the material and are frequency dependent. The η_r can be calculated by

$$\eta_r = (1 - |\Gamma|^2) \tag{1.17}$$

When the mismatching efficiency is considered during the calculation, the calculated antenna gain is called the realised gain ($G_{realised}$). This is the overall efficiency of the antenna. Another method to define the antenna efficiency is to use the effective aperture, and the antenna efficiency is defined as the ratio of the effective area aperture to the actual physical size of the antenna

$$\eta = \frac{A_{eff}}{A} \tag{1.18}$$

where A represents the physical aperture size and A_{eff} represents the effective aperture size of the antenna. The A_{eff} can be calculated by

$$A_{eff} = \frac{\lambda^2}{4\pi} G \tag{1.19}$$

1.2.3 Polarisations

The polarisation of an antenna is defined as the polarisation of the wave radiated by the antenna [1]. Depending on the orientation of the electric field, the polarisation of the antenna can be classified as linearly polarised, circularly polarised or elliptically polarised.

Assume a plane wave travelling in the $-z$ direction, which can be written as

$$\vec{E}(z,t) = \vec{x}E_{x0}\cos(\omega t + kz + \phi_x) + \vec{y}E_{y0}\cos(\omega t + kz + \phi_y) \tag{1.20}$$

where E_{x0} and E_{y0} are the maximum magnitudes of the x and y components, respectively. The antenna is linearly polarised if the phase difference between these two components is 180° or

$$\Delta\phi = |\phi_x - \phi_y| = n\pi, n = 0, 1, 2, \ldots \tag{1.21}$$

If the amplitudes of the x and y components are the same while the phase difference $\Delta\phi$ is 90°, the antenna is circularly polarised

$$\Delta\phi = |\phi_x - \phi_y| = n\pi/2, n = 1, 3, 5, \ldots \tag{1.22}$$

$$E_{x0} = E_{y0} \tag{1.23}$$

For a circularly polarised wave, the electric vector at a given point in space traced as a function of time is a circle. The sense of rotation can be determined by observing the direction of the field's rotation as the wave is viewed along the direction of propagation. If the rotation is clockwise, the wave is right-hand circularly polarised (RHCP). If the field rotation is anti-clockwise, the wave is left-hand circularly polarised (LHCP).

If the amplitudes of the x and y components are not equal but the phase difference $\Delta\phi$ is 90°, then the antenna is elliptically polarised

$$\Delta\phi = |\phi_x - \phi_y| = n\pi/2, n = 1, 3, 5, \ldots \tag{1.24}$$

$$E_{x0} \neq E_{y0} \tag{1.25}$$

For the elliptical polarisation, the electric vector traced at a given position is a tilted ellipse, as shown in Figure 1.7. In practice, it is impossible to obtain a pure circularly polarised antenna within the entire bandwidth of the antenna. Thus, the term axial ratio (AR) is defined to describe how circular the radiated wave is. It is defined as the ratio of the major axis to the minor axis of the ellipse [1]

$$AR = \frac{OA}{OB} \tag{1.26}$$

where OA represents the major axis and OB represents the minor axis of the ellipse. These can be calculated by using the following equations

$$OA = \left[\frac{1}{2}(E_{x0}^2 + E_{y0}^2) + [E_{x0}^4 + E_{y0}^4 + 2E_{x0}^2E_{y0}^2\cos(2\Delta\phi)]^{1/2}\right]^{1/2} \tag{1.27}$$

$$OB = \left[\frac{1}{2}(E_{x0}^2 + E_{y0}^2) - [E_{x0}^4 + E_{y0}^4 + 2E_{x0}^2E_{y0}^2\cos(2\Delta\phi)]^{1/2}\right]^{1/2} \tag{1.28}$$

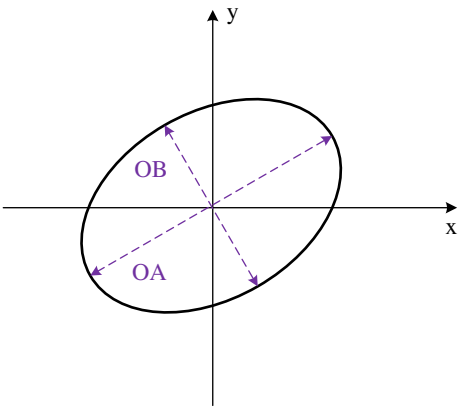

Figure 1.7 Tilted ellipse of elliptical polarisation.

The tilt angle of the ellipse relative to the y axis is

$$\tau = \frac{\pi}{2} - \frac{1}{2}\tan^{-1}\left[\frac{2E_{x0}E_{y0}}{E_{x0}^2 - E_{y0}^2}\cos(\Delta\phi)\right] \tag{1.29}$$

AR is an important parameter of a circularly polarised antenna. Normally it is required that the AR of a circularly polarised antenna at the frequency band of interest is below 3 dB. In some applications, such as satellite communications, the requirement for the AR is more rigorous. For a circularly polarised antenna, it is important to check both the impedance and AR bandwidth, as they do not necessary overlap in the same frequency range. As an example, Figure 1.8a shows the impedance and AR bandwidth of a circularly polarised patch antenna. The AR is taken at the angle $\theta = 0^\circ$ where the maximum gain of the patch is. This patch is a probe-fed square patch and has resonance at 7.9 GHz. The patch is corner truncated in order to obtain circular polarisation. Figure 1.8b shows the layout of this circularly polarised patch. The AR minimum is at 7.5 GHz and the AR ($AR < 3$) bandwidth partially overlaps with the impedance bandwidth of the patch.

Besides the bandwidth, another important parameter for a circularly polarised antenna is the AR beamwidth. The AR beamwidth describes the coverage region where the radiated waves from the antenna are circularly polarised. Figure 1.9 shows the simulated radiation pattern of the circularly polarised patch at its resonance in the $\phi = 0^\circ$ plane. As shown, the dominant polarisation of this patch is RHCP and the 3 dB beamwidth of the patch is 80° (from −40° to +40°). The 3 dB AR beamwidth corresponds to the angle range where the LHCP is 15 dB lower than RHCP, which is from −31° to +85°. Thus, the overlapped HPBW and AR beamwidth is from −31° to +40°.

1.3 Antenna Array Fundamentals

An antenna array consists of multiple antenna elements positioned within an aperture. The total radiation pattern of an array antenna is the vector addition of the field radiated by each radiating element, and it can be expressed as the product of the array factor (AF) times the radiation pattern of the isolated radiating element. Each array element is excited by the input RF signal with certain amplitude and phase. By controlling the

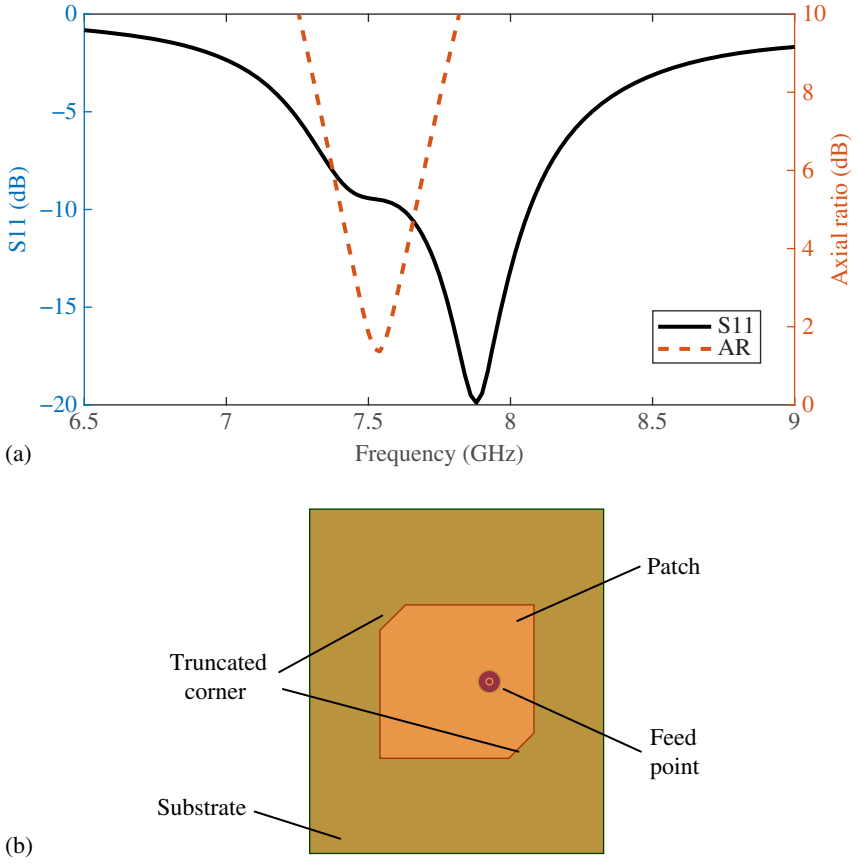

Figure 1.8 (a) The return loss and AR of a patch antenna. (b) The layout of the corner truncated square patch.

excitations of the array antenna, the beams of the array antenna can be formed to provide constructive interference to the desired direction and form nulls at undesired directions.

The array antenna is a critical component of the smart antenna. It determines the beam-steering performance (e.g. the largest beam scanning angle), directivity, and radiation efficiency of the antenna system. The BFN and the microwave circuit determine the beam-steering or beam-switching capability of the array antenna. The antenna array can be either a linear array or a planar array. The linear array is an array of antennas placed along one axis, as shown in Figure 1.10. A number of identical elements are spaced by a distance d and excited with phase difference β. Assuming that these elements are excited by identical amplitudes, the array factor can be derived as [1]

$$AF = \sum_{n=1}^{N} e^{j(n-1)\psi} \tag{1.30}$$

where $\psi = kd\cos\theta + \beta$ and θ is the scan angle of the array antenna.

Besides the linear array configuration, antenna elements can also be placed along a rectangular grid to form a planar array, as shown in Figure 1.11. Planar arrays are more flexible in beamforming and, ideally, the main beam can be steered to any desired

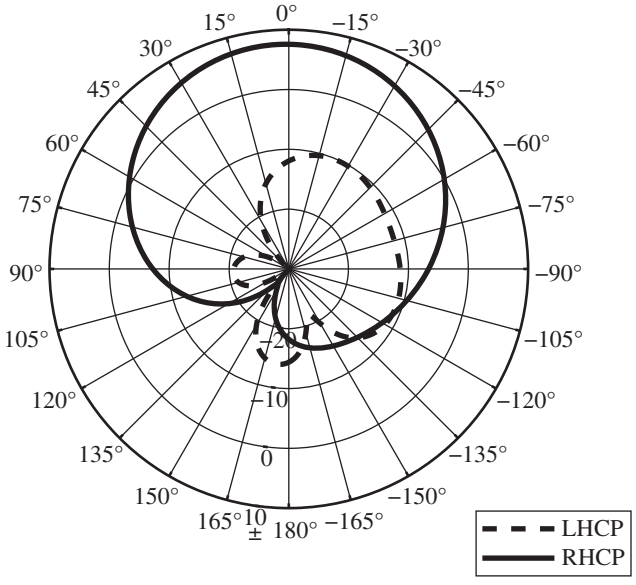

Figure 1.9 The simulated radiation pattern of the circularly polarised patch at its resonance in the $\phi = 0^\circ$ plane.

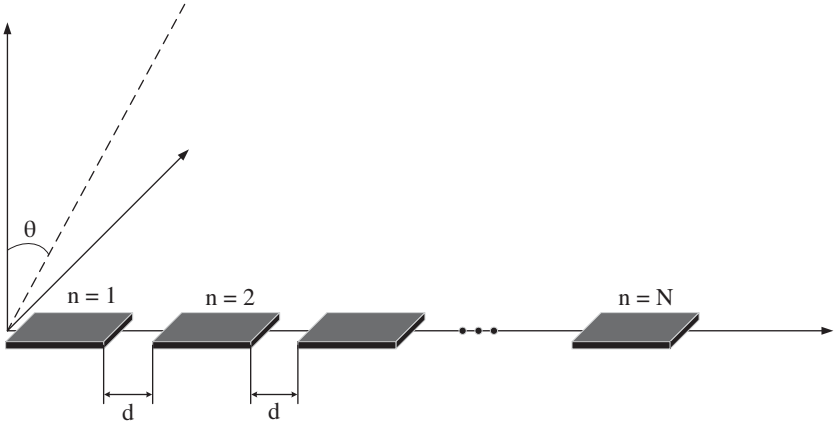

Figure 1.10 Linear array configuration.

direction (θ, ϕ). Thus, in general, the planar array is preferred for the design of smart antennas so it can benefit from the advanced BFN and signal processing algorithm. The array factor of the planar array can be written as [1]

$$AF = S_{xm} S_{yn} \tag{1.31}$$

where

$$S_{xm} = \sum_{m=1}^{M} e^{j(m-1)(kd_x \sin\theta \cos\phi + \beta_x)} \tag{1.32}$$

$$S_{yn} = \sum_{n=1}^{N} e^{j(n-1)(kd_y \sin\theta \sin\phi + \beta_y)} \tag{1.33}$$